Advanced Review

Electronic structure of conducting organic polymers: insights from time-dependent density functional theory

Ulrike Salzner*

Conducting organic polymers (COPs) became an active field of research after it was discovered how thin films rather than insoluble infusible powders can be produced. The combination of the properties of plastics with those of semiconductors opened the research field of organic electronics. COPs share many electronic properties with inorganic semiconductors, but there are also major differences, e.g., the nature of the charge carriers and the amount of the exciton binding energy. Theoretical analysis has been used to interpret experimental observations early on. The polaron model that was developed from one-electron theories is still the most widely used concept. In the 1990s, time-dependent density functional theory (TDDFT) became available for routine calculations. Using TDDFT, electronic states of long oligomers can be calculated. Now UV spectra of neutral and oxidized or reduced species can be compared with in situ UV spectra recorded during doping. Likewise states of cations can be used to model photoelectron spectra. Analysis of states has resolved several puzzles which cannot be understood with the polaron model, e.g., the origin of the dual absorption band of green polymers and the origin of a 'vestigial neutral band' upon doping of long oligomers. DFT calculations also established that defect localization is not crucial for spectral changes observed during doping and that there are no bound bipolarons in COPs.

How to cite this article:
WIREs Comput Mol Sci 2014. doi: 10.1002/wcms.1194

INTRODUCTION

Saturated organic polymers that have revolutionized material science in the 20th century are electrical insulators. In contrast, conducting organic polymers (COPs) are unsaturated hydrocarbons with alternating single and double bonds. Delocalization of the π-electrons gives rise to semiconductor-like energy bands and electric conductivity once mobile charge carriers are produced by electronic excitation, oxidation, or reduction. The smaller energy gap between occupied and unoccupied π-orbitals compared with that between σ-orbitals, leads to absorption and emission of visible light. The unique combination of electrical and optical properties with the processibility of plastics can be used to produce devices such as all-plastic electrical wires, transparent conductors, batteries, organic solar cells also known as organic photovoltaics (OPVs), organic field effect transistors (OFETs), integrated circuits, organic light-emitting diodes (OLEDs), sensors, and image processors.[1–3]

Probably the first electrochemical synthesis of a COP, polyaniline (PAN), has been achieved in 1862.[4] Optical[5] and electronic[6] properties of conjugated π-systems have been studied in the 1930s, and chemical and electrochemical doping were reported in the 1960s.[6–9] The major breakthrough in COP research, however, started with an accident.[1] Molar instead of millimolar quantities of Ziegler catalyst was

*Correspondence to: salzner@fen.bilkent.edu.tr
Department of Chemistry, Bilkent University, Ankara, Turkey
Conflict of interest: The author has declared no conflicts of interest for this article.

used in the polymerization of acetylene, which resulted in copper- and silver-colored shiny films instead of the usual infusible, insoluble black powders.[10] The silvery film of polyacetylene resembled the golden appearance of $(SN)_x$ and led to collaboration among Hideki Shirakawa, Alan McDiarmid, and Alan Heeger. Their joint publication in 1977[11] reporting conductivity increase of polyacetylene (PA) by seven orders of magnitude on oxidation with iodine, initiated enormous research efforts around the world and culminated in the Nobel Prize to the three researchers in 2000.

Because PA is chemically unstable, a huge amount of synthetic work has been carried out since 1977 to produce COPs with better stability and properties tailored for specific applications.[12–14] Examples of homopolymers, PAN, PA, polythiophene (PTH), polypyrrole (PPY), polyfuran (PFU), polyparaphenylenevinylene (PPV), polyethylenedioxythiohene (PEDOT), and polyfluorene (PFL) are shown in Scheme 1. Side chains can be introduced to improve solubility and crystalline order.[15] PEDOT is the first COP that found commercial application.[16] It is standing out because of its chemical stability, small band gap, and electrochromic properties. In recent years, the focus has shifted from homo- to copolymers. Combination of electron-donating and electron-accepting units such as 4-(dicyanomethylene) -4*H*-cyclopenta[2,1-*b*:3,4-*b*¢]dithiophene (CDM),[17] benzothiadiazole (BT),[18] and diketopyrrolopyrrole (PYPY)[19] (Scheme 2) allows band gap manipulation[20] and has proven to be particularly suitable for applications in OPV devices.[21]

Having a large variety of different systems available, it is important to understand how changes in molecular structure influence electronic properties and device performance. The most important properties that have to be controlled for devices such as OFETs, OPVs, and OLEDs are ionization potential (IP) and electron affinity (EA), efficiency of charge carrier injection and charge carrier collection at electrodes, electron and hole mobility, light absorption and emission, exciton diffusion rate, charge carrier generation and separation at interfaces, purity and morphology of thin films, and morphological and thermal stability.[22] To realize the full potential of COPs in organic electronics, experimental and theoretical research approaches have been combined from the beginning. Theoretical methods

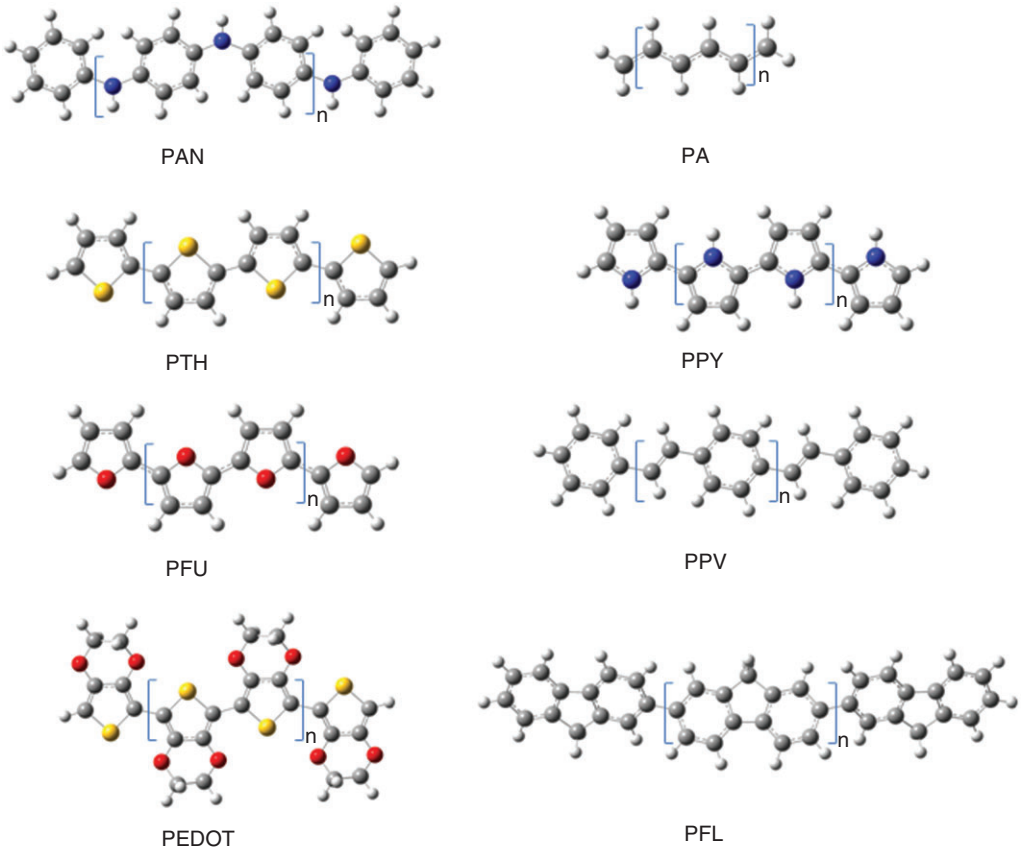

SCHEME 1 | Structures of typical COPs.

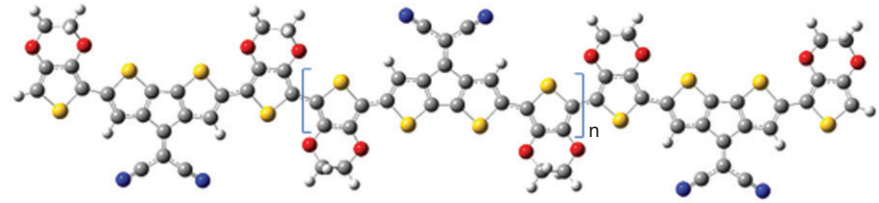

PEDOT-CDM-EDOT

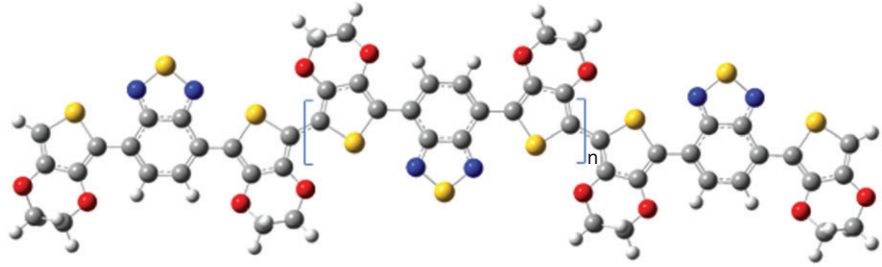

PEDOT-BT-EDOT

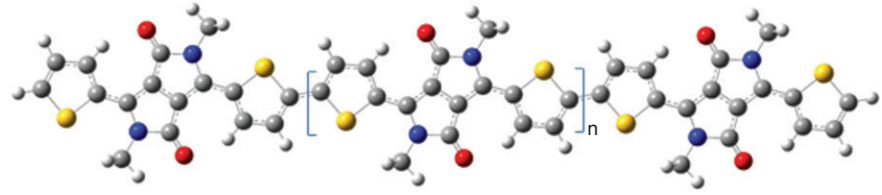

PTH-PYPY-TH

SCHEME 2 | Structures of donor–acceptor systems.

applicable to the complex properties of these large systems have developed along with the improvements in computer hardware. To a first approximation, properties of anisotropic COPs can be investigated on isolated polymers or oligomers. For isolated species, density functional theory (DFT) and time-dependent DFT (TDDFT) have led to important insights and accurate predictions. Such investigations are the focus of this review. Intermolecular interactions can be assessed with three-dimensional band structure calculations or via cluster models. Ultimately, predicting device performance requires also modeling of morphology, i.e., crystal structures including their defects as well as charge carrier dynamics at interfaces. These are fields of research that are gaining momentum but are beyond the scope of this overview.

ION STATES, BAND STRUCTURES, AND ORBITAL ENERGIES

Band Structures

Electronic properties of COPs are determined by the energy levels of their electrons. High-energy valence electrons are associated with low IPs, low-lying unoccupied levels with high EAs. Close-lying electronic states lead to high charge-transfer rates, and widely spaced electronic energy levels are indicative of high charge carrier mobility. The simplest way of analyzing electronic structures of metals and semiconductors theoretically is with band structure calculations. Band structures of solids are obtained by defining a repeat unit and the unit cell size, and carrying out the calculations on infinite systems with periodic boundary conditions.[23] Band structures can be calculated in one, two, and three dimensions. To a first approximation, COPs are one-dimensional systems with anisotropic properties.[24] Therefore, one can start an investigation of isolated infinite chains, neglecting interchain interactions. Alternatively, finite systems of increasing chain lengths and extrapolation can be employed to approach properties of polymers.[25,26] With large oligomers or clusters, molecular orbital energies can be used in the same way as band structures. The similarity of the two approaches that only appear to be different because of the different terminology used by physicists and chemists has been demonstrated by Hoffmann.[27,28]

Photoelectron Spectra

The electronic structure of COPs can be determined experimentally with photoelectron (PES),[29] inverse photoelectron spectroscopy (IPES), and two-photon photoemission (2PPES).[30,31] The basic principle of photoelectron spectroscopy is that the binding energy of an electron equals the energy difference between the corresponding state of the cation and the neutral species. PES experiments generate all possible ion states that can be reached with a given light source and measure the kinetic energy distribution of the ejected photoelectrons. The most intense PES peaks are usually associated with removal of a single electron from the ground state of the molecule. More complex ion states are observed as satellites.[29] Because relaxation of the electron cloud on electron removal or addition occurs instantly on the PES time-scale, relaxation is part of the measured IPs. Geometric relaxation is slower and may be included[30] or excluded[29] in the measurement. In the solid state, there is an additional relaxation due to the molecular environment. The electronic influence of the environment, the so-called-solid state polarization energy, has been determined experimentally to lower IPs of organic π-systems by a rather constant value of around 1.7 eV compared with the gas-phase values.[32] Solid-state polarization increases EAs but the exact amount has not been measured as accurately as for IPs. Therefore, the solid-state polarization energy for EAs is usually assumed to be the same as that for IPs.[30] The lattice relaxation of the nuclei is too slow to be seen in PES.[30]

Orbital Energies

The relationship between electron binding energies and orbital energies of the neutral species as obtained with band structure calculations is provided by Koopmans's theorem,[33] which states that negative Hartree–Fock (HF) orbital energies are the IPs and EAs of the system. The relationship is mathematically exact but neglects electronic relaxation because the orbitals of the neutral species differ from those of the cations. Electronic relaxation is actually quite large.[29] Koopmans's theorem works well at the HF level for gas-phase IPs and especially for the negative energy of the HOMO ($-E_H$) because errors due to relaxation and correlation cancel partially. For lower-lying orbitals, the relationship deteriorates because of increasing correlation effects. For EAs, relaxation and correlation errors add up so that Koopmans's theorem is useless for EAs at the HF level. Unless three-dimensional band structure or cluster calculations are performed at theoretical levels that account for polarization,[34] orbital energies also neglect the solid state polarization energy.

Modeling solid-state PES[35,36] and IPES[37] spectra with semi-empirical CNDO/S3 and INDO gas-phase calculations was successful after aligning of the highest occupied molecular orbital (HOMO) and lowest unoccupied molecular orbital (LUMO) energies with the experimental first IP and EA and by empirically adjusting band widths. Hückel theory, which is strictly a one-electron approach, does not include electron-electron interactions self-consistently and produces the same orbital energies for cations, neutral species, and anions. Thus, within Hückel theory, orbital energies are IPs and EAs but electron repulsion is missing when an electron enters a half-occupied orbital.

In recent years, DFT has almost completely replaced semi-empirical and ab initio methods because it is the most accurate approach that can be applied to large-size systems such as COPs. However, the interpretation of DFT orbital energies is complicated.[38] There is evidence that $-E_H$ corresponds to the relaxed first IP with the unknown exact density functional.[39–41] All other orbital energies were originally considered to be meaningless,[41] because in DFT orbitals are used to construct the electron density rather than to minimize the energy. The situation is aggravated by the fact that the exact density functional is unknown and that the many different approximate functionals produce very different orbital energies. Nonetheless, it was apparent from the beginning that despite these shortcomings, relative DFT orbital energies produce reasonable band structures that are actually in better agreement with experiment than those obtained at the HF level for which the meaning of orbital energies is well defined.[42–45] More recent theoretical analyzes have revealed the underlying reasons for the success of DFT orbital energies in electronic structure theory.[38,46–48]

The quality of DFT orbital energies depends strongly on the approximate functionals that fall into three groups, pure DFT, global hybrid functionals, and range-separated hybrids. The nature of exchange and correlation functionals within each of the three groups makes relatively little difference. Pure DFT underestimates the first IP, overestimates the EA, and therefore underestimates band gaps. Energy levels lie generally too close, so that band widths are also underestimated. These problems arise from the lack of a derivative discontinuity in the exchange-correlation potential.[38] Another important issue is the self-interaction error (SIE) that is not canceled completely in DFT because exchange is calculated only approximately.[41,49] Energies of localized orbitals have larger errors than that of delocalized ones, so that relative energy levels of

π- and σ-electrons are also incorrect.[38] Global hybrid functionals with 20-30% of HF exchange improve on relative orbital energies but first IPs remain several eV too small.[38,42] After the orbital energies are shifted, so that the $-E_H$ energy matches the first IP, all other orbital energies agree with higher IPs with global hybrid functionals[38] (Figure 1 bottom). Agreement with experiment without empirical adjustment can only be achieved, however, when the self-interaction error is removed, e.g., with the statistical averaging of model orbital potentials (SAOP)[46,47] or with range-separated hybrid functionals (Figure 1 top) that use no or little short-range HF exchange (close to the nucleus) and 100% of long-range HF exchange (at larger distance from the nucleus).[50–52] An additional issue with DFT is that all properties depend too strongly on system size. Thus, the decrease in IPs with increasing oligomer length is overestimated which means that IPs of long oligomers and polymers are too low, even with functionals that predict IPs of small molecules correctly.[53] This problem can also be addressed with certain range-separated hybrid functionals.[54]

A special kind of range-separated hybrid functionals are the so-called 'γ-tuned' range-separated hybrids,[55–57] where γ is a flexible parameter that determines at which distance from the nucleus the amount of HF exchange starts to increase. γ-tuning is based on the above mentioned exact relationship between $-E_H$ and the relaxed IP with the unknown exact density functional. Because ΔSCF IPs (total energy differences between cations and neutral forms) are usually predicted accurately by DFT methods and because $-E_H$ depends more strongly on γ than ΔSCF IPs, γ can be adjusted so that $-E_H$ and ΔSCF IP match. Once this is achieved for a system, the γ-tuned density functional is used to obtain all other properties. It was shown that many shortcomings of approximate functionals can be overcome with γ-tuning.[56–59] For oligomers with increasing chain lengths, problems arise, however.[54] As chain lengths increase, the DFT ΔSCF IPs tend to become too small. This could in principle be counteracted by increasing γ (using 100% HF exchange at shorter distance from the nucleus). However, matching $-E_H$ and ΔSCF IP requires decreasing γ for oligomers with increasing chain lengths so that $-E_H$ and ΔSCF IP can no longer be matched. The interesting conclusion from this is that the SIE that is usually considered to be the main error in DFT cannot be the reason for the problems of DFT with increasing system size. Because SIE is smaller for delocalized orbitals than for localized ones,[60] it should decrease with increasing length in contrast to what is observed.

Ion States

With the development of TDDFT,[61–64] which can be applied to large oligomers with several hundred atoms, it became possible to calculate states directly and reassess the accuracy of orbital energies without reference to experiment. TDDFT is applicable to neutral systems, and to radical cations and anions, so that electronic and geometric relaxation, and electronic excitation on doping can be investigated independently. As mentioned previously, the first IP can be calculated with the ΔSCF method as the energy difference between energies of neutral molecule and cation. The higher IPs can be obtained with TDDFT by calculating excited states of the cations, selecting the states that correspond to the ions that have the hole in the appropriate orbitals (i.e., the states that transfer β-electrons from lower-lying orbitals to the semi-occupied molecular orbital (SOMO)), and adding the excitation energies to the first IP.[51,53] Comparison of excited state energies of cations with orbital energies has revealed that DFT with certain range-separated hybrid functionals produces accurate orbital energies for valence and innervalence electrons down to around −30 eV.[51,53]

A particularly suitable functional for large π-systems is wB97XD.[54,65] For 4-thiophene, gas-phase IPs[66] were predicted at wB97XD/6-311G* level with orbital energies and states showing errors of less than 0.2 eV.[54] In Figure 1, orbital energies and states are compared with experiment for 8-thiophene at wB97XD/6-311G* and B3LYP/6-311G* (all figures in this article are based on results obtained using Gaussian 09[67]). Experimental peak positions and heights are obtained from Table 1 in the study by de Silva Filho et al.[66] Orbital energies were given peak heights of 1, and states are given peak heights corresponding to the square of the coefficient of the dominant electron configuration in the cation state. A coefficient of close to 1 indicates that a peak is due to a single electron removal, small coefficients indicate strong correlation. At the wB97XD/6-311G* level without γ-tuning, $-E_H$ of 8-T is 6.96 eV and the ΔSCF IP is 6.76 eV. Thus, negative orbital energy and ΔSCF IP differ by only 0.2 eV. Both values compare well with the experimental IP of 6.84 eV. The strong feature at around 9 eV that was deconvoluted into two peaks[66] actually arises from 10 close-lying orbitals. Errors increase for higher IPs, overestimating them by about 0.4 eV. Thus, the band width is somewhat overestimated. This is not the case for 4-T.[54] Therefore, a trend to overestimate band widths with increasing chain length becomes apparent. The PE spectrum at the B3LYP/6-311G* level had to be aligned because $-E_H$ would predict an IP of only 5.04 eV and the

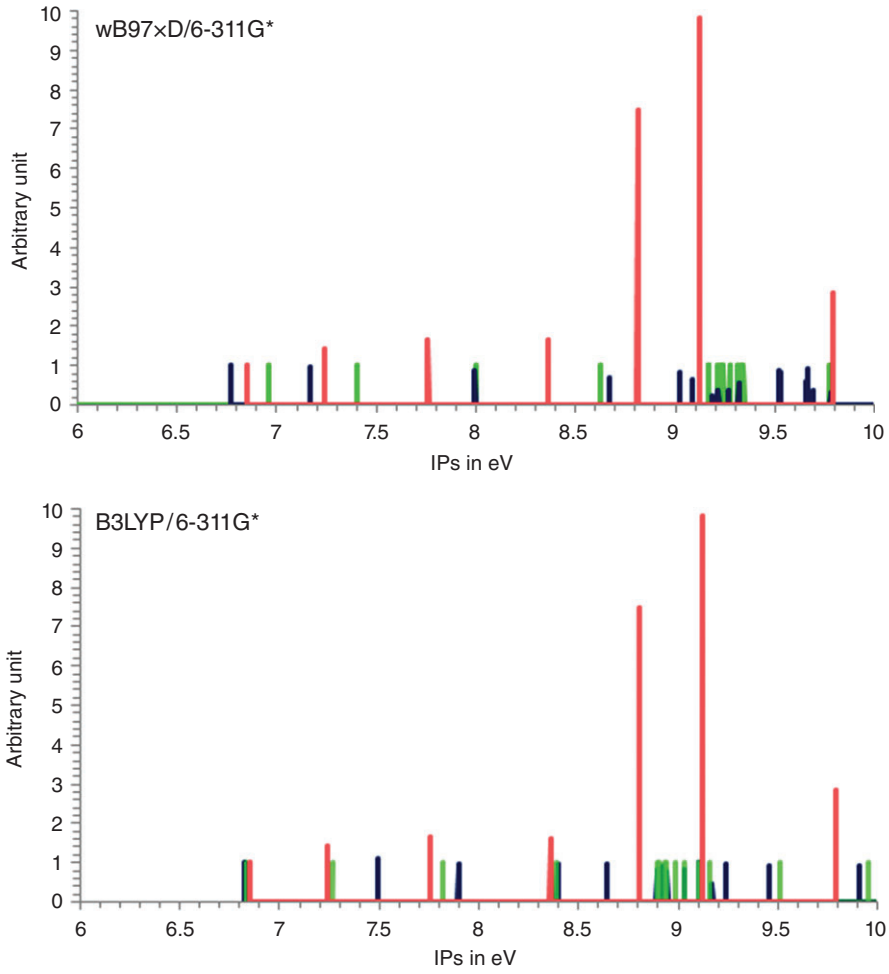

FIGURE 1 | Gas-phase IPs (red), orbital energies (green), and ion-state energies (blue) of 8-thiophene.

ΔSCF IP is 5.95 eV. After individually aligning $-E_H$ and the ΔSCF IP with the experimental first IP, B3LYP spectra are in good agreement with experiment and the band width is overestimated less than with the wB97XD functional, showing that relative energy levels are very accurate with global hybrids.

To obtain solid-state band structures, the solid-state polarization energy needs to be evaluated theoretically. This has been carried out with a small cluster of five 6-thiophene oligomers.[54] The wB97XD functional is suitable for this type of calculation because it includes dispersion and accounts for polarization effects that are absent with most density functionals.[34] The difference in the first IP between gas-phase molecule and cluster is about 0.9 eV ($-E_H$: 0.79 eV, ΔSCF $IP_{vertical}$: 0.88 eV, ΔSCF $IP_{adiabtic}$: 0.99 eV). If the vertical IP is used for the molecule in the gas phase but the adiabatic IP for the cluster as suggested in Ref 30 the solid-state polarization energy amounts to 1.37 eV. This approaches the measured value of 1.7 eV.[32] The EA increases in the cluster by around 0.3-0.5 eV ($-E_H$: 0.29 eV, ΔSCF $EA_{vertical}$: 0.41 eV, ΔSCF $EA_{adiabatic}$: 0.49 eV). The difference between the vertical gas-phase and the adiabatic solid-state EA is 0.86 eV. Therefore, the solid-state polarization effect on the EA is substantially smaller than that on the IP, in contrast to previous assumptions.[30]

The close resemblance of energies of cation states and orbital energies with range-separated hybrid functionals shows that DFT orbital energies can be employed to predict band structures.[51] Knowing that orbital energies are reliable with appropriate choice of the density functional is extremely useful for research on COPs because determining IPs by calculating inner valence states requires inclusion of hundreds of excited states, which is impossible for very long oligomers and polymers. The term 'bands' will be used also in the following for oligomers although an oligomer 'band' contains only as many states as there are repeat units in the oligomer. Figure 2 compares orbital energy band structures of typical homo- and donor-acceptor co-oligomers with 24 conjugated

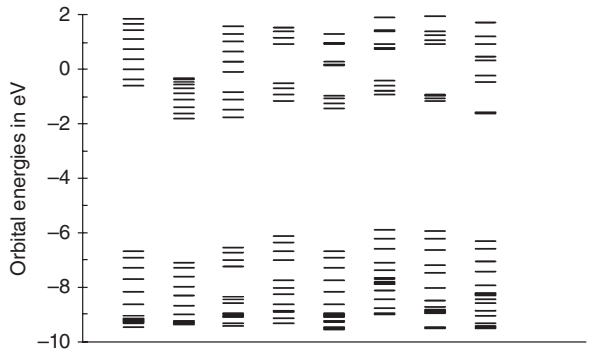

FIGURE 2 | Twenty occupied and 10 unoccupied molecular orbital energies of systems with 24 conjugated double bonds: 12-TH, 12-BT, 4-TH-PYPY-TH, 4-PY-PYPY-PY, 4-TH-BT-TH, 4-EDOT-BT-EDOT, 4-PY-BT-PY, and 3-EDOT-CDM-EDOT at wB97XD/6-31G*.

double bonds at wB97xd/6-31G*. Homo-oligomers 12-TH and 12-BT have continuous conduction bands. Donor-acceptor systems have a tendency to form separate states that are localized on the acceptor as seen by the four energy levels below the conduction bands.[68] The degree of localization is reflected in the closeness of the four energy levels and depends on acceptor and donor. The least localization is observed with the PYPY acceptor (third and fourth column) and the strongest with CDM (last column). The difference in localization between PYPY and BT systems (columns 5-7) cannot be attributed to LUMO energy or EA differences because both monomers have very similar LUMO energies, PYPY −0.49 eV and BT −0.54 eV. In contrast, the LUMO of CDM lies much lower at −1.76 eV. With the same acceptor, band widths depend on the donor. In general, PY decreases conduction band widths more than TH because the high-lying LUMO of PY interacts less with the low-lying LUMOs of the acceptors. The consequences of localization in conduction bands with donor-acceptor systems for optical spectra are discussed in the next chapter.

BAND GAPS

One of the early issues regarding polyenes was whether there is a band gap at infinite chain length or, in other words, whether PA is a metal or a semiconductor. The crucial parameter turned out to be bond length alternation (BLA).[69–71] BLA lifts the degeneracy between HOMO and LUMO of infinite PA and therefore opens up a gap, which depends on the degree of BLA. For COPs other than PA, HOMO and LUMO are not degenerate even without BLA but the amount of BLA still contributes to the band gap. As BLA remains a determining factor for the size of band gaps COPs,[26] accurate determination would be desirable. Unfortunately, different levels of theory predict quite different single- and double-bond lengths. It was shown for instance for 6-T with the 6-311G* basis set that HF overestimates BLA by underestimating double-bond lengths and overestimating single-bond lengths. Second-order perturbation theory is accurate for single bonds but overestimates double-bond lengths, pure DFT overestimates both but double bonds more. Usage of HF exchange in global hybrids tends to shorten double bonds, leading to relatively accurate results for BLA. Range-separate hybrids depending on the amount of long-range HF exchange and on the range separation parameter tend to get too close to the HF results.[54] Comparison of bond length in the thiophene monomer at CCSD/6-311G* and MP2/6-311G* reveals that the main reason for the large differences in theoretical results is that the associated energy differences are very small. For instance, CCSD/6-311G* and MP2/6-311G* predict quite different BLA values, 0.068 Å and 0.040 Å, respectively but recalculation of the energy with CCSD at the MP2 geometry led to an increase by only 0.04 kcal/mol.[53]

Band gaps are related to optical absorption, to the difference between electrochemical oxidation and reduction potentials, and to the difference between IP and EA. Because measurements of these properties are performed under different conditions and involve different physical processes, band gaps obtained from optical absorption (E_g), cyclic voltammetry (E_{CV}), and PES (E_t) differ (Box 1). In the gas-phase, E_t is much larger than the optical gap E_g. In condensed phases, E_g may be smaller or larger than in the gas phase depending on solvent effects and crystal packing. For COPs, the difference between gas-phase and condensed-phase E_g values is usually not larger than 0.4 eV and often much smaller. Due to the solid-state polarization energy on IP and EA, E_t is much smaller in the solid state than in the gas phase.[30] The same holds true for solutions. As a result, condensed phase E_ts from PES and IPES or E_{CV} can be very close to E_g (within 0.4 eV). As described previously, the relationship between band structures or orbital energies and physical states is Koopmans's theorem or its analog in DFT. Thus, theoretical band or HOMO-LUMO gaps correspond to E_t. HOMO-LUMO gaps from gas-phase calculations should therefore be much larger than E_g.

HF orbital energy differences overestimate E_t because of their failure to produce reasonable EAs. Pure DFT leads to much too small band gaps because IPs are underestimated and EAs are overestimated. Including HF exchange with hybrid functionals increases E_t compared with pure DFT. The strongest

BOX 1

BAND GAP

The term band gap comes from solid-state physics and refers to an energy range in a solid where no electron states exist. Theoretical band gaps are used to interpret UV-Vis spectra, PE spectra, and oxidation and reduction potentials from cyclic voltammetry. In organic materials, the values obtained with these approaches may differ substantially.

OPTICAL BAND GAP

UV spectroscopy measures the energy that is required to excite an electron from the top of the valence to the bottom of the conduction band. The electron and the hole left behind attract each other electrostatically, forming a bound electron-hole pair or exciton.

TRANSPORT GAP

PES measures the energy required to remove electrons from the valence band, whereas IPES measures the energy released when an electron is introduced into the conduction band. The energy difference between them is the transport gap. Transport and optical gap differ by the exciton binding energy which is large in the gas phase but reduced in the condensed phases.

ELECTROCHEMICAL BAND GAP

With cyclic voltammetry, the difference between oxidation and reduction potentials is measured in solution. Therefore, the electrochemical band gap is conceptually closer to the transport gap than to the optical gap.

THEORETICAL BAND GAPS

The optical gap can be calculated as the energy difference between ground and first excited state. The transport gap can be obtained as the difference between the ionization energy and the electron affinity calculated with the ΔSCF method. Only the transport gap can be approximated with HOMO and LUMO orbital energies.

point of range-separated hybrid functionals is that they predict accurate orbital energies and therefore correct E_ts. An oddity of hybrid functionals with about 20-30% of HF-exchange is that they produce gas-phase HOMO-LUMO gaps that are very close to E_g[42,45] although orbital energy differences do clearly not account for exciton binding and polarization energies. This has led to wide-spread use of gas-phase DFT HOMO-LUMO gaps as estimates for polymer E_gs and E_{CV}s, and the method has proven to be quite useful[72] although it is strictly speaking comparing 'apples with pears'.

Modeling UV Spectra

The first experiments carried out on conjugated systems, polyenes and organic dyes, were actually measurements of their UV spectra. In the 1930s, it was already established that light absorption of conjugated π-systems shifts to longer wavelength with increasing number of conjugated double bonds and that the red shift is accompanied by increasing intensity. Explicit consideration of excited states was not possible at the time and excitation energies were approximated with orbital energy differences. With Hückel theory, Mulliken[5] was able to prove that the strong absorption is in general an $N->V_1$ band and that weaker higher energy bands are transitions to higher vibrational levels. Because of its strict one-electron nature, Hückel theory cannot be applied to two electron processes and fails to account for fluorescence quenching by low-lying two-photon states in extended polyenes.[73] Extensive experimental work on polyenes in the 1970s and 1980s produced vibrationally resolved gas-phase and solution spectra. The difference between the onset of absorption of C_8H_{10} and $C_{12}H_{14}$ in gas and condensed phases is around 0.4 eV depending on solvent, concentration, and chain length of the polyene.[74,75]

High-quality spectra of medium-sized systems are useful for assessing accuracy of theoretical methods. Vibrationally resolved UV spectra have been analyzed theoretically and were used to establish the relationship between onset of absorption and vertical excitation energy as produced by TDDFT.[76,77] Figure 3 shows the vibrationally resolved spectrum of $C_{12}H_{14}$ at TDwB97XD/6-31G*. The line shape is practically identical to that observed experimentally. The energy of the 0-0 transition is underestimated by 2400 cm^{-1} or 0.30 eV. At B3P86-30%/6-31G*, the spectrum appears identical but is shifted to lower energy, so that the error in the 0-0 transition energy is 0.5 eV.

The general practice is to use vertical excitations because calculating vibronic spectra requires excited-state frequencies that have to be obtained numerically. This is extremely time-consuming and therefore not practical for large systems. Figure 3 shows that the three main vibrational peaks lay within about 4000 cm^{-1} or about 0.5 eV. The difference between E_{0-0} and E_{vert} is 0.38 eV at wB97XD/6-31G* and 0.28 eV at B3P86-30%/6-31G*. As most

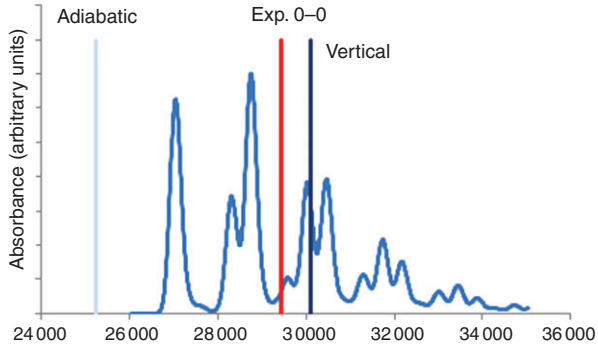

FIGURE 3 | Vibronically resolved main absorption peak of $C_{12}H_{14}$ at wB97XD/6-31G*. The dark blue line indicates the vertical excitation; the light blue line represents the adiabatic excitation energy; and the red line denotes the experimental value from Ref 75.

functionals underestimate excitation energies, some error cancelation occurs by using E_{vert}. Additional uncertainties arise from incorrect chain length dependence and solvent effects. The solvent effect of CH_2Cl_2 on the vertical excitation energy of $C_{12}H_{14}$ calculated with the polarized continuum model as implemented in Gaussian 09[67] is 0.22 eV at wB98xd/6-31G*. This is only about half of the experimental value. For larger systems, solvent effects appear to decrease. For 19-FU, for example, PCM predicts a solvent effect of only 0.04 eV (compare Figure 6). Although solvent effects are therefore not a major issue, current theory is far from the accuracy that would be necessary for predicting the colors of organic π-systems and agreement between theory and experiment of better than around 0.4 eV is aided by fortuitous error cancelations. With these cautionary remarks in mind, trends predicted by comparing different π-systems are usually quite accurate because electronic structures of different COPs are very similar from a theoretical point of view. From this point forward, vertical excitations will be discussed exclusively.

Dependence of Vertical Excitation Energies on Structure and Chain Length

Homopolymers

Theoretical E_{vert} values calculated with TDDFT of polyenes, thiophene, pyrrole, furan, and many other oligomers with increasing chain length reproduce the single strong feature in the visible region of COPs and confirm that this excitation is dominated by a single absorption during which an electron is transferred from HOMO to LUMO. Figure 4 shows spectra of BT oligomers with 2-12 repeat units as examples. With increasing chain length, the strong absorption shifts to lower energy and increases in intensity, and the contribution of the HOMO-LUMO transition decreases while HOMO-1→LUMO+1, HOMO-2-LUMO, and HOMO-LUMO+2 excitations start to contribute. Apart from different peak positions, excitation spectra of all homo-oligomers appear similar.

Donor-Acceptor Systems

Figure 5 compares spectra of donor-acceptor systems with PYPY, BT, and CDM acceptors and of 12-TH. With PYPY as the acceptor, spectra show a prominent peak and weaker features at higher energy. Compared with 12-TH, the main peak is strongly red-shifted and an additional weak band appears at 3.3 eV. With BT, the high energy absorption is stronger. The energy difference between the first and second peak and its intensity can be influenced with the donor. As donor strength increases in the order TH < EDOT < PY, the high energy absorption is blue-shifted and becomes stronger, so that for 4-PY-BT-PY, the peak heights are about the same. The 'camel back' absorption was first discovered experimentally and gives rise to green polymers.[78] It is therefore very important for completing the color spectrum of COPs. The nature of the double absorption was puzzling at first as it is not predicted with the polaron model (see below). It was first rationalized for FL copolymers with ZINDO semi-empirical calculations.[79] The occurrence of two absorptions rather than one is a direct consequence of the difference in band structures between donor-acceptor systems and homopolymers[68] (Figure 2). The low energy transition arises from a charge-transfer (C-T) state from the HOMO to the lowest localized acceptor level. Although it is a HOMO-LUMO transition, it has a very different character than the $\pi-\pi^*$ transition in homopolymers. The second absorption peak is a transition where the electron jumps over the localized acceptor states into the delocalized π^* orbitals of the conjugated system.[79] This analysis is fully confirmed with TDDFT.[80] The localization is strongest with CDM as the acceptor and consequently the oscillator strength is shifted almost completely to the second absorption. The total oscillator strengths of the two bands displayed in Figure 5 sums up to about 4.5. As the second band increases in intensity, the first decreases, fulfilling the Thomas–Reiche–Kuhn sum rule.[81]

Thus, the donor-acceptor concept has more complicated implications than expected when it was suggested at first. Originally the idea was to produce small band-gap polymers with wide conduction bands.[20] Especially the CDM systems show that the latter claim does not hold and that the small band gap comes at the price of low electron mobility[17] caused by localization.[82] With respect to device performance, the

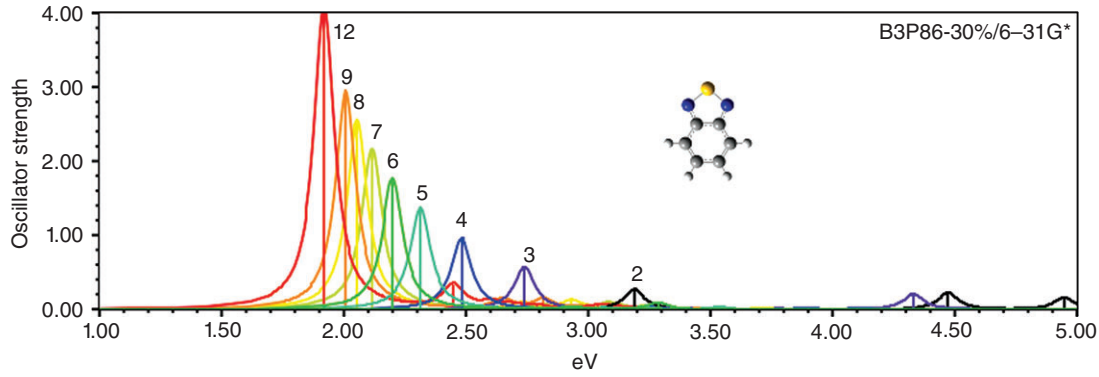

FIGURE 4 | UV spectra of 2-BT through 12-BT at B3P86-30%/6-31G*.

different behavior is clearly reflected in the experimental applications. CDM is rarely used. PYPY systems have but little C-T character in the low energy UV-absorption band and a low-lying wide conduction band. These systems have exceptionally large electron mobilities,[83] which is a requirement for OFETs. Donor-acceptor polymers with BT have dual absorption in the visible part of the spectrum and are among the most successful systems as donors for OPVs.[84] As in bulk heterojunction solar cells,[85] electron transport is provided by the acceptors (usually fullerenes) following charge transfer, the small conduction band widths of BT systems are not detrimental in OPV applications.

CHARGE CARRIERS IN COPS

In their neutral states, COPs are semiconductors with band gaps between about 1 and 4 eV. Therefore, they are insulating at room temperature. Electronic excitation, oxidation, or reduction, are necessary to generate mobile charge carriers. Oxidation has resulted in the highest conductivities by far, 10^5 S/cm[86] in the case of PA and around 2×10^3 S/cm for PTH[87] and PPY.[88] Although oxidation and reduction processes are referred to as doping, they differ from doping in inorganic semiconductors. Being organic molecules, changes in electronic structure of COPs are associated with structural relaxation so that charge transport is coupled to geometric distortion. Hückel theory[89] and its solid-state analog, the Su–Shrieffer–Heeger Hamiltonian[90] approach predict that the charge carriers in PA are different from those of most other COPs. PA has a degenerate ground state in the sense that exchanging the positions of single and double bonds leads to a new structure with the same energy as the original one. In neutral PA with structural defects, partially delocalized boundaries between the two forms exist, which explain the existence of paramagnetic defects (solitons) in undoped PA.[90] If charges are added or removed during doping, positively and negatively charged solitons result (Scheme 3 left).

Polymers with Nondegenerate Ground States

In polymers with nondegenerate ground states[91] such as PPY and PTH, single bond–double bond flipping leads to a higher energy structure and a quinoid segment (Scheme 3 right). After doping, experiments on PPY and PTH had revealed that conductivity of COPs correlates with doping level but not with the strengths of ESR signals[92] and therefore not with the concentration of free charge carriers, the nature of the charge carriers in COPs moved to the center of attention.[93]

Conductivity in the absence of free spins can be rationalized with Landau's polaron model for a charge moving through a crystal.[94] A 'polaron' is the combination of displacement of atoms and polarization of their electron clouds by a charge.[95] The extent of the distortion can be estimated by representing the effect of the charge by its force acting on a lattice vibration in the harmonic oscillator approximation. Localization or delocalization of the polaron depends on two opposing factors, the kinetic energy of the electrons favoring delocalization and lattice relaxation favoring localization of the polaron.[95] In the presence of two charges, lattice relaxation favors two charges to share the same distorted lattice site. If lattice relaxation energy and dielectric screening are large enough, Coulomb repulsion between the two like charges may be overcome and 'bipolarons' may result. Therefore, binding of two like charges to one another can occur as a consequence of saving lattice distortion energy.

In heterocyclic COPs such as PTH and PPY, oxidation or reduction causes disruption of the bond alternation scheme and geometry changes (Scheme 3 left). The transition between aromatic and quinoid forms in polymer chains is taken as the analog of

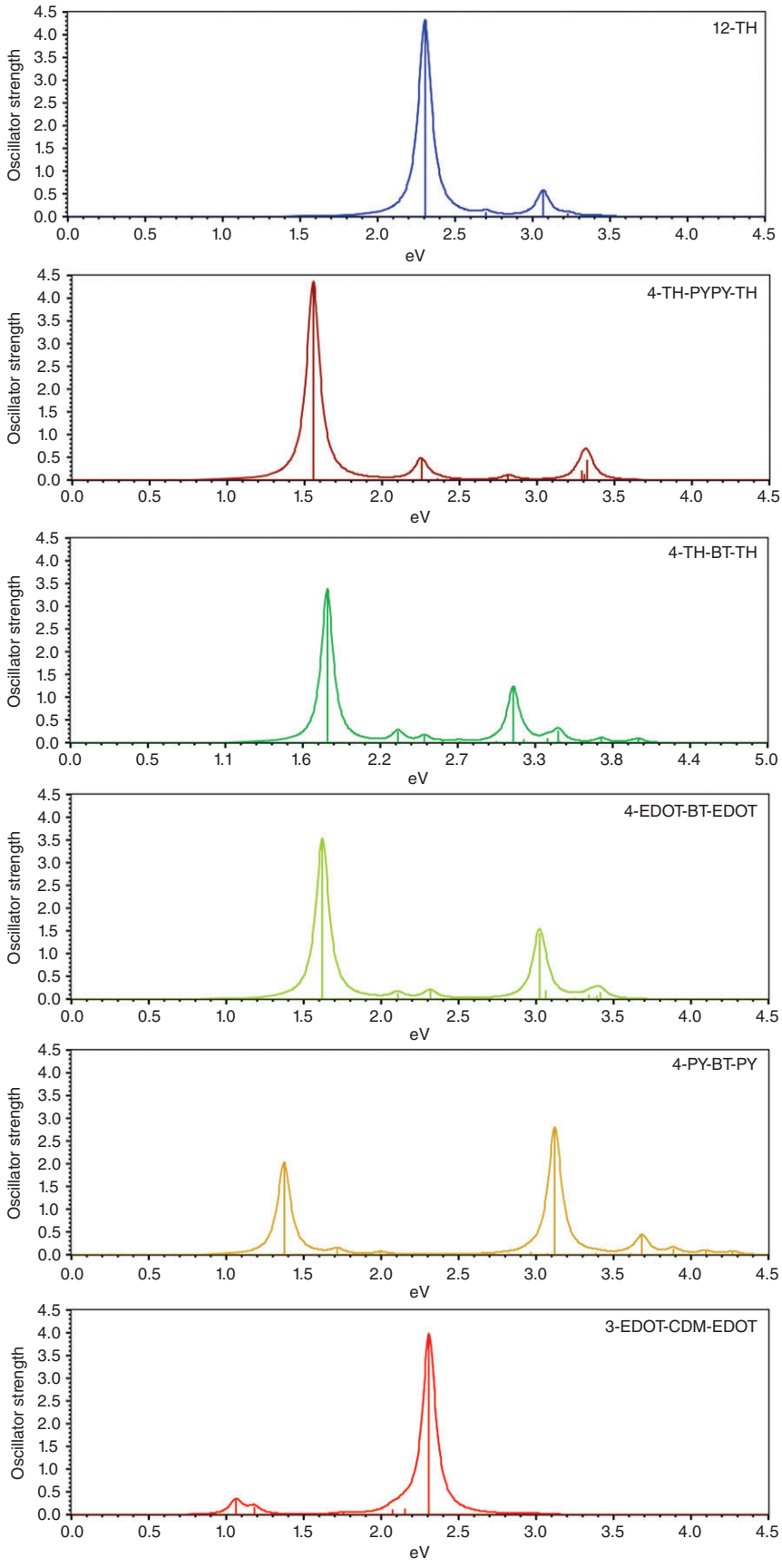

FIGURE 5 | TDB3P86-30%/6-31G* UV spectra of donor–acceptor systems with 24 conjugated double bonds.

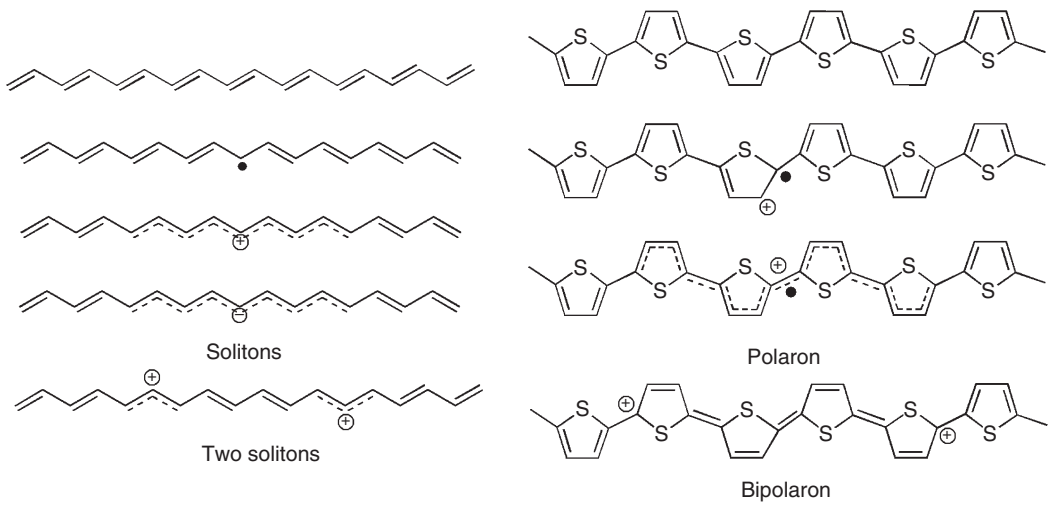

SCHEME 3 | Defects caused by free radicals and charges in COPs.

the lattice distortion in the crystal of the polaron model.[91,93] Because quinoid have higher energies than aromatic forms[54] (for neutral polymers), two charges were expected to stay at close distance to keep the high energy quinoid chain segment short. Therefore, two charges are predicted to form a spinless bound bipolaron,[93] explaining the lack of correlation between number of free spins and conductivity.

The doping process can be followed by in situ UV spectroscopy. On oxidation or reduction, the intensity of single absorption peak of the neutral species vanishes and two sub-gap bands develop.[96,97] These spectroscopic features have been rationalized with the polaron model invoking electronic transitions between valence and conductions bands, and localized intragap polaron levels.[93,98] With one-electron theories, solitons are predicted to give rise to one, polarons to three, and bipolarons to two sub-gap transitions.[98] Therefore, early theoretical analysis of the two sub-band transitions in in situ UV spectra supported the hypothesis that charge carriers in COPs with nondegenerate ground states are bipolarons.

Experimental Results on Oligomers in Solution

Objections to these conclusions were raised when doping behavior of oligomers in dilute solution was investigated.[99–101] With oligomers, chain lengths and doping levels are well defined, while neither of them is certain in electrochemically produced polymers. Experiments on medium-sized oligomers with 3–8 thiophene rings showed identical spectral changes upon doping as seen in thin-film experiments, but revealed that two sub-gap transitions are associated with singly charged species rather than with dications. Therefore, the two peaks in singly oxidized thin films suggest that charge carriers in COPs are polarons and not bipolarons. On addition of a second equivalent of dopant, a single sub-gap peak was observed. Rarely mentioned is another interesting observation. For longer oligomers (>8 rings), the absorption band of the neutral species decreases upon doping with one equivalent of dopant to about half its intensity but does not vanish.[102–104] This 'neutral absorption'[103] band was taken as evidence for formation of two independent polarons on one oligomer in a single oxidation step, leaving half of the oligomers in their neutral state.[102] Alternatively the 'vestigial neutral band' was considered evidence of polaron localization, leaving neutral chain segments that absorb at similar energy as the neutral species.[103]

Polaron Size and Bipolaron Binding Energy

The crucial questions regarding the charge carriers in COPs are the sizes of polarons and the possible presence of bound bipolarons. These two questions have been studied for over 30 years but no consensus has been reached. In principle, one can address the problem by optimizing structures of neutral and charged oligomers and by comparing to what extent structural parameters and charge distributions differ from those of the neutral analogs. The issue of bipolarons versus two polarons can be addressed by structural optimization of dications with open-shell and closed-shell approaches. Which species is present can be decided by analyzing whether one or two defects are lower in energy. The reason why a generally accepted conclusion has not been reached is that results depend strongly on the level of theory. Interactions between

charges (electrons or holes) that are at the heart of the problem are dealt within the two-electron part of the Hamiltonian, which is exactly that part that all practical quantum mechanical methods are approximating. In the early 1980s, when computer resources were much more limited than nowadays, semi-empirical methods were the only choice. Extended Hückel theory (EHT) and its solid-state physics version, the SSH method are one-electron theories that include interaction between electrons only via experimental parameters. For charged species, both methods predict polaron widths of about five rings and bipolaron binding energies of 0.34 eV in PPP and 0.45 eV in PPY.[93,105] However, investigating interactions between charge carriers with one-electron theories that do not include electron–electron interactions self-consistently, is the worst choice of method for the problem.[106–108]

Hartree–Fock (HF) theory is also a one-electron method but it includes electron–electron interactions at least approximately and self-consistently. HF methods were developed for polymers in the 1960s[109] and applied to COPs routinely in the 1980s.[110,111] Second-order perturbation theory corrections were employed as early as 1983.[112] The problem of all HF-based approaches is that correlation between electrons of same spin is included (exact exchange), but correlation between electrons of opposite spin is entirely neglected. The resulting unphysical preference of the HF method for high spin states is detrimental for calculations of extended open-shell π-systems. Polarons, which are radical cations or anions, should have expectation values of the S^2 operator of 0.75. Unrestricted Hartree–Fock (UHF) calculations, however, produce values well above seven for long polyene radicals and predict over-delocalized defects.[113] In contrast, restricted open-shell Hartree–Fock (ROHF) calculations that enforce the correct S^2 value, confirm the localized nature of defects[113] and the strong bipolaron binding found with SSH. Semi-empirical calculations in the restricted open-shell formalism come to very similar conclusions as ROHF.[106]

DFT and TDDFT Analysis of Charge Carriers

DFT includes correlation approximately and does not calculate exchange exactly. As a result, electronic interactions between electron pairs with same and with opposite spin are treated in a balanced way, which practically eliminates the problem of spin contamination for large π-conjugated radicals. However, the approximation of the exchange leads also to the biggest disadvantage of DFT, the SIE. This problem has been shown to lead to wrong prediction of charge-transfer excitations[114] and incorrect dissociation of radical cations into half-electron states.[115,116] Such unphysical results show that some caution is warranted when using DFT calculations to assess the nature of the charge carriers in COPs. Three-dimensional band structure calculations within the local density functional approximation (LDA) underestimate BLA in PA and do not predict any defect localization.[117] In oligothiophenes bipolarons dissociate into separate polarons.[107]

Hybrid functionals with 20–30% of HF exchange improve on the problems of pure DFT substantially. These functionals produce reasonable BLA[45] and with the exception of polyene radicals[118] there is very little spin contamination in long singly charged oligomers as long as the HF exchange contribution does not exceed around 30%.[119] A careful comparison of spin distributions in medium-sized polyene radicals showed that the B3LYP hybrid functional is in quite reasonable agreement with coupled cluster theory, overestimating hydrogen coupling constants somewhat.[113] Defect sizes on odd-numbered polyene radical cations with the B3P86-30% functional agree with MP2 results for oligomers with 41 CH units. For oligomers with up to 101 CH units, large defects spreading over 80 CH units are predicted.[118] In thiophene oligomer with up to 25 rings, defects spread over the whole molecule. Defect sizes are very sensitive to the presence of counter ion and solvent because relatively large structural changes are associated with small energy differences.[119] As an example, Figure 6 depicts bond-length differences between neutral 19-FU and its cation optimized in the gas phase and in CH_2Cl_2 at the B3P86-30%/6-31G* and wB97XD/6-31G* levels of theory. Including solvent effects changes the defect shape at B3P86-30%/6-31G* dramatically. Whereas the defect is completely delocalized in the gas phase, bond-length changes are most prominent in the middle of the molecule in the presence of solvent. The energy difference between the two structures is, however, only 0.91 kcal/mol. The energy difference between the gas phase and solvent structures with wB97XD/6-31G* is even smaller, 0.33 kcal/mol. This demonstrates the structural flexibility of doped COPs and explains the large difference in defect sizes obtained with different theoretical methods. Closed-shell and open-shell calculations with global hybrid functionals on dications are in agreement with pure DFT and do not produce bound bipolarons.

Range-separated[50,56] hybrid functionals decrease polaron sizes to about 10–15 rings in the gas phase and to less than 10 in solution (Figure 6), but confirm

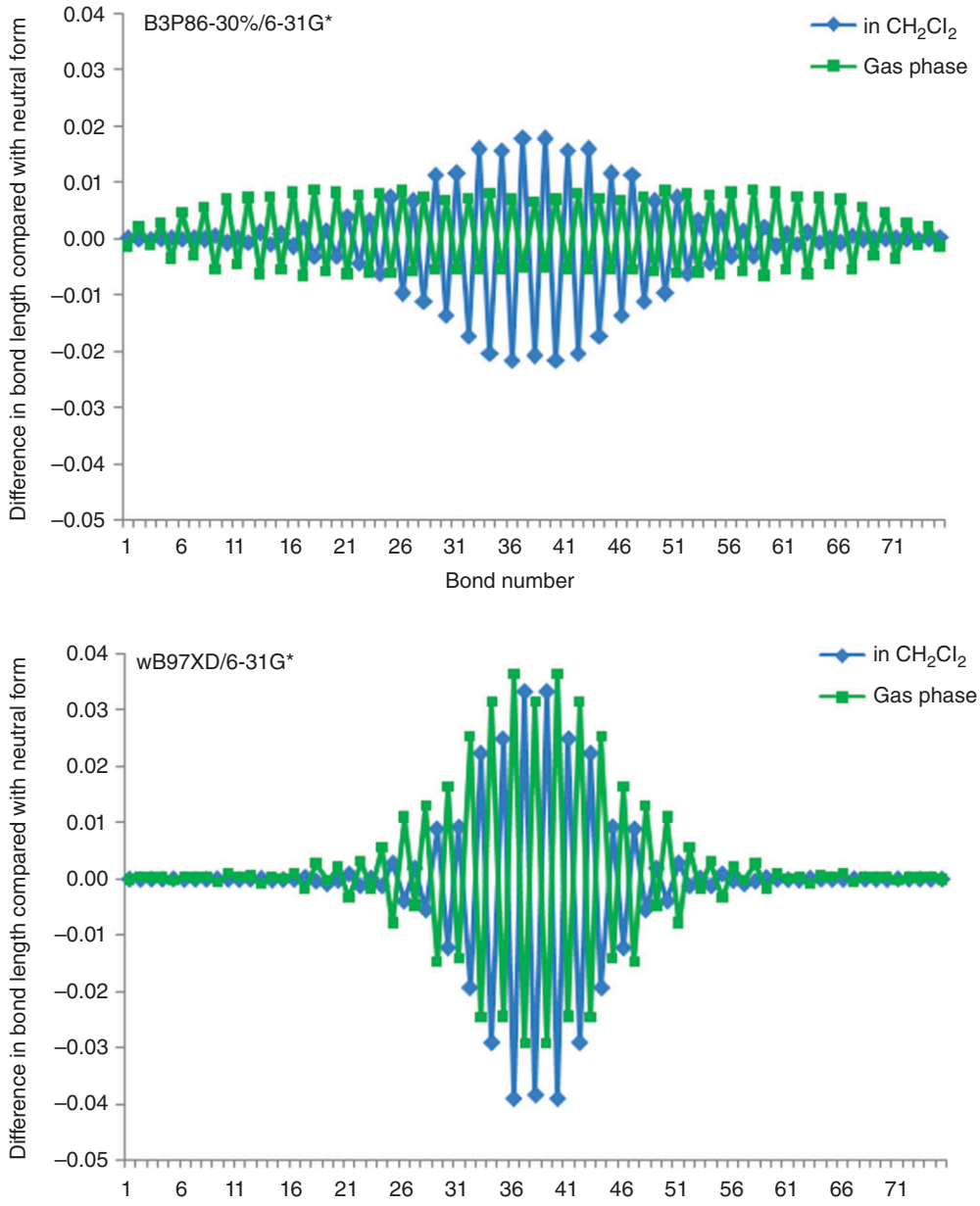

FIGURE 6 | Bond-length differences between of 19-FU neutral form and cation in gas phase and in CH_2Cl_2 at B3P86-30%/6-31G* and wB97XD/6-31G*.

the absence of bound bipolarons.[54] As discussed previously, range-separated hybrid functionals are also capable of removing problems with incorrect chain-length dependence of band gaps and ionization energies of neutral species. However, they reintroduce the spin contamination problem for open-shell systems because of the large amount of HF exchange at long range. Expectation values of the spin operator for radical cations reach around 0.8–1.0 depending on the functional and range-separation parameter. Generally around 10% overestimation or values of ≤0.83 are considered acceptable. Consequently, problems with open-shell systems and with higher excited states are emerging.[54] Thus, a single-density functional for calculating all relevant properties of COPs remains elusive. Using coupled cluster theory would be desirable but cannot be performed for systems of sufficient size to establish polaron sizes and bipolaron-binding energies. Therefore, DFT is currently the only reasonable choice. At all levels of DFT, polarons structures are very flexible and bipolarons are unstable. Only multiply charged systems[120] have bipolaron-like structures when polarons overlap because there is not enough space for them to separate.

UV Spectra of Doped Systems

An indirect method to address the issue of polaron size and bipolaron formation is calculating UV spectra of cations and dications as closed-shell (bipolaron) and open-shell (two polarons) species and comparing them to experiment. TDDFT spectra of mono cations and anions are almost identical[121] and display therefore perfect electron hole symmetry. Medium-sized singly charged oligomers exhibit two sub-band transitions as observed experimentally. Thus, TDDFT calculations confirm that the two sub-band transitions developing during doping of thin films are polaron and not bipolaron states. To investigate the effect of geometry on cation spectra, the spectrum of the 6-TH cation was calculated with the slightly nonplanar gas-phase geometry of the neutral species and after full optimization of the cation. As shown in Figure 7, sub-band absorptions are obtained with cation structure, only band shape or position change. Therefore, electronic structure changes and not geometrically localized defects are responsible for the spectral changes on doping.[119,122]

The lower energy transition is due to a HOMO-1→SOMO transition of a β-electron and the higher energy band is due to a HOMO–LUMO transition of an α-electron.[119,122] For the vertical cation, the splitting of the higher energy band is caused by mixing with electronic transitions involving lower-lying occupied orbitals. With increasing chain length of the oligomers, the low energy transition increases in intensity until the increase levels off at chain length of around eight rings. At that chain length, the second band starts loosing intensity and a third band at the position where the neutral species absorbs, develops. For very long oligomers (>20 rings), the third peak dominates the spectrum and the second band has almost vanished[54,119,122] (as shown for TH oligomers at the B3P86-30%/CEP-31G* level in Figure 8). The shift in oscillator strength from the second to the third band is in line with the Thomas–Reiche–Kuhn sum rule.[81] The same behavior is predicted for FU, FL, and PY oligomers.

As mentioned previously, the additional absorption at the neutral band position has been observed experimentally for TH and FL oligomers.[102–104] Because the polaron model does not predict such a band, the persistence of the neutral band was puzzling and has led to the contradictory claim that 12-TH oxidizes upon doping with one equivalent of dopant in a single step to the dication, leaving half of the oligomers in their neutral form. This rationalization accounts for the remaining absorption at the neutral band position but does not explain why the dications form. The bands in the spectra are clearly polaron and not bipolaron bands, so that they indicate that there is no bipolaron binding energy. In the absence of a bipolaron binding energy, however, there is no driving force for dication formation. Theoretical results resolve the contradiction in revealing that long oligomer cations have three absorption bands and that neutral species are not involved in this absorption.

Figure 8 shows also the spectra of open-shell dications. Whereas closed-shell dications have only one low energy band, dications of longer oligomers that are more stable as open-shell species (two polarons rather than a bipolaron) have two absorption bands at higher energy than the corresponding cation. This explains the experimentally observed shift of the two polaron bands to higher energy on adding a second equivalent of dopant.[102] Thus, the theoretical spectra in Figure 8 fully explain the observed spectral features during doping of 12-TH[102] in terms of polarons at low, and unbound overlapping polarons at high doping levels.

As defects size is strongly influenced by the presence of counter ions[119,122,123] and solvents (Figure 6), it is an interesting question to which extent the strong absorption at the position of the neutral band is influenced by the environment and whether spectra reach

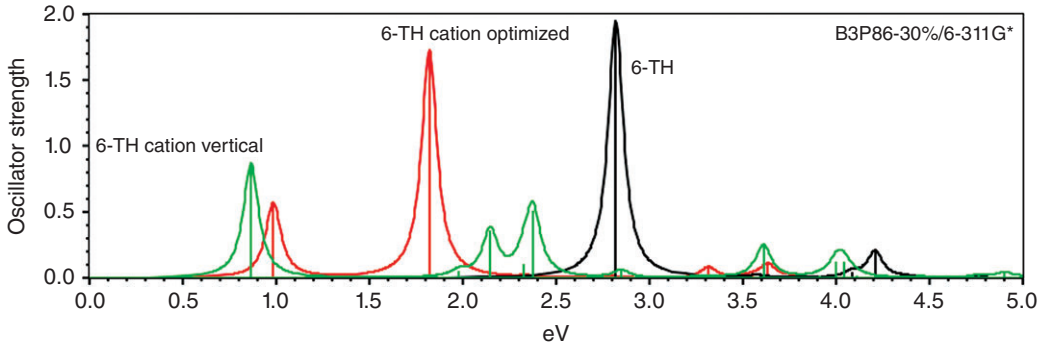

FIGURE 7 | UV spectra of 6-TH, and 6-TH$^+$ without (vertical) and with optimization of the cation structure.

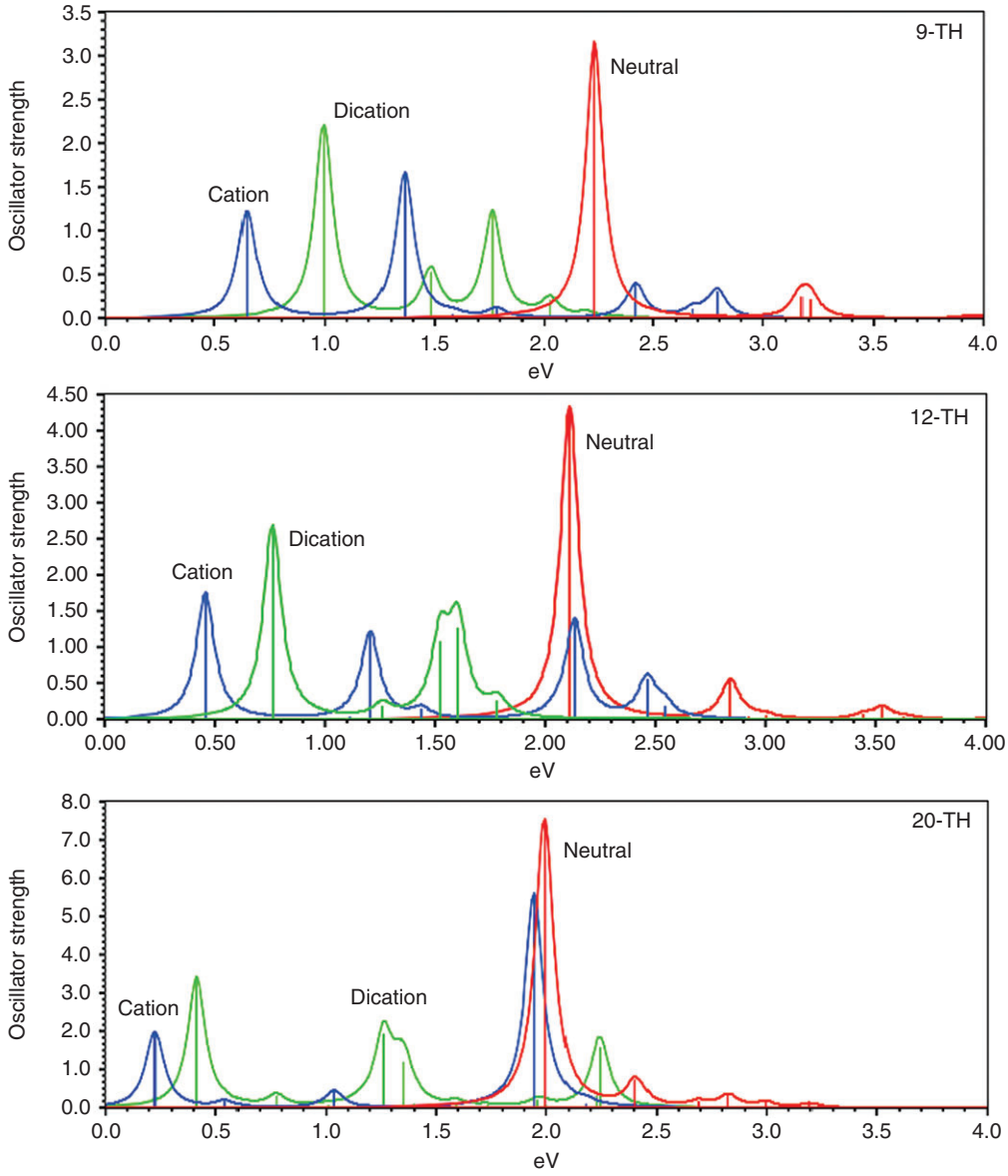

FIGURE 8 | Development of UV spectra of oligomers with increasing chain length.

convergence with respect to chain length of oligomers with localized defects. Figure 9 shows spectra of 19-FU at B3P86-30%/6-31G* and wB97XD/6-31G* in the gas phase in methylene dichloride. The four cation structures span the whole range from completely delocalized (B3P86-30%/6-31G* gas phase (Figure 6)) to localized defect over only seven rings (wB97XD/6-31G* in CH_2Cl_2). Despite the very different cation structures the spectral features are essentially the same. Localization merely moves the cation band that occurs close to the neutral absorption to slightly higher energy. This confirms that electronic structure and not defect localization is responsible for sub-band transitions and hence the 'vestigial neutral band' is a cation feature that does not require neutral chain segments.

CONCLUSION

DFT and TDDFT can both be applied to oligomers that are long enough to address crucial properties of COPs. To predict reasonable structures and electronic properties, inclusion of HF exchange is necessary. With global hybrids, the amount of HF exchange should be around 30% to obtain reasonable BLA and to correct the problems with overestimating chain-length dependence of properties at least partially. Among range-separated hybrids, those

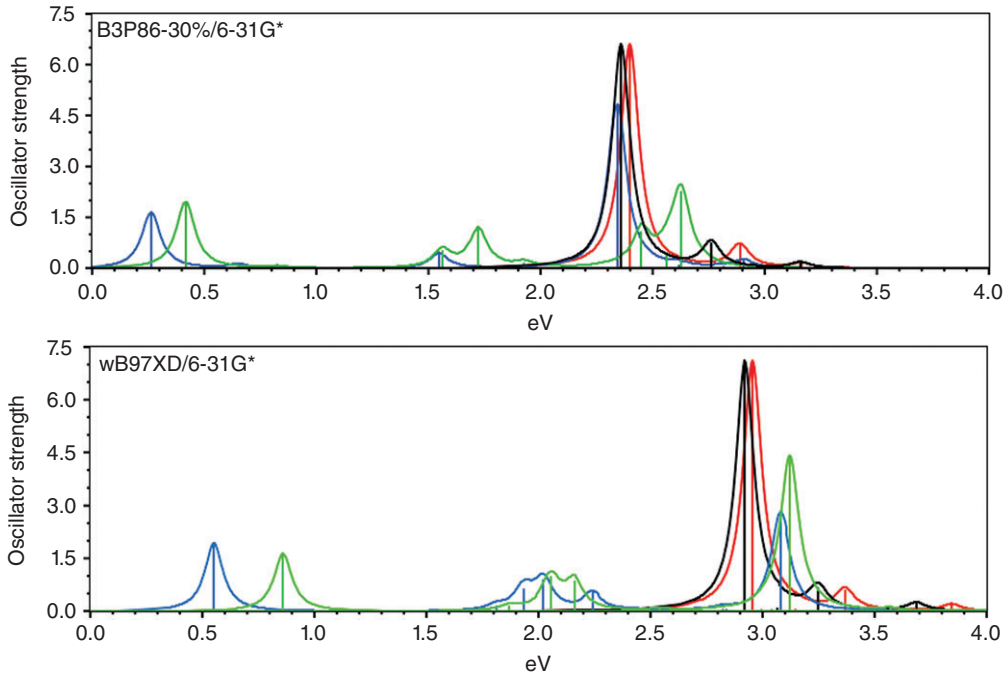

FIGURE 9 | Cation spectra of 19-FU at B3P86-30%/6-31G*and wB97XD/6-31G* in gas phase and in CH_2Cl_2.

functionals that include short-range HF exchange such as wB97XD are most suitable. Global hybrids are somewhat superior to radical cations and higher excited states, range-separated hybrid are better for properties of long neutral systems. Trends among different polymers are well reproduced with either type of functional.

Calculation of states with TDDFT reveals that the polaron model is insufficient in several respects. The emphasis on defect localization originating from one-electron theories is unjustified as energy differences between structures with localized and delocalized defects are very small and because spectral changes on doping are reproduced independently of defect localization in the cations. Thus, studies on transport and charge carrier dynamics should take this flexibility into account. The polaron model further fails to account for the occurrence of an additional absorption band in UV spectra of doped oligomers with more than about 18 conjugated double bonds. These absorptions arise from mixing of close-lying electronic configurations which cannot be accounted for with single-electron theories. Likewise the dual-band absorption of certain donor–acceptor systems and the relative intensities of the two peaks are beyond to polaron model. DFT methods with any density functional contradict the existence of bound bipolarons and the agreement between TDDFT spectra of open-shell dications with experimental spectra corroborates the conclusions based on the energetic preference. It is therefore recommended to abandon the polaron model and to switch to easily applied TDDFT.

TDDFT studies on single molecules and molecular clusters have reached a level of maturity that guaranties reliable predictions. Device modeling starts with defining sets of desirable values for parameters such as, for instance, IPs, EAs, and excitation energies, which can be provided easily. The next step in predicting device performance must be to include morphology prediction and to improve understanding of charge-carrier dynamics at interfaces. This kind of research is currently undergoing major progress and valuable insights are expected to emerge in the near future.

ACKNOWLEDGMENT

The authors thanks TUBITAK grant TBAG-109T426 for funding this work.

REFERENCES

1. Shirakawa H. The discovery of polyacetylene film: the dawning of an era of conducting polymers (Nobel lecture). *Angew Chem Int Ed Engl* 2001, 40:2575–2580.
2. MacDiarmid AG. "Synthetic metals": a novel role for organic polymers (Nobel lecture). *Angew Chem Int Ed Engl* 2001, 40:2581–2590.
3. Heeger AJ. Semiconducting and metallic polymers: the fourth generation of polymeric materials (Nobel lecture). *Angew Chem Int Ed Engl* 2001, 40: 2591–2611.
4. Letheby H. XXIX.—on the production of a blue substance by the electrolysis of sulphate of aniline. *J Chem Soc* 1862, 15:161–163.
5. Mulliken RS. Intensities of electronic transitions in molecular spectra VII. Conjugated polyenes and carotenoids. *J Chem Phys* 1939, 7:364–373.
6. Becher M, Mark HF. Polymere als elektrische Leiter und Halbleiter. *Angew Chem* 1961, 73:641–646.
7. Bolto BA, McNeil R, Weiss DE. Electronic conduction in polymers. III. Electronic properties of polypyrrole. *Aust J Chem* 1963, 16:1090–1103.
8. Bolto BA, Weiss DE. Electronic conduction in polymers. II. The electrochemical reduction of polypyrrole at controlled potential. *Aust J Chem* 1963, 6:1076–1089.
9. McNeil R, Siudak R, Wardlaw JH, Weiss DE. Electronic conduction in polymers. I. The chemical structure of polypyrrole. *Aust J Chem* 1963, 16:1056–1075.
10. Shirakawa H. Twenty-five years of conducting polymers. *Chem Commun* 2003:1–4.
11. Shirakawa H, Louis FJ, MacDiarmid AG, Chiang CK, Heeger AJ. Synthesis of electrically conducting organic polymers: halogen derivatives of polyacetylene, (CH)x. *J Chem Soc Chem Commun* 1977:578.
12. Skotheim TA. *Handbook of Conducting Polymers*. New York: Marcel Dekker; 1986.
13. Skotheim TA, Elsenbaumer RL, Reynolds JR, eds. *Handbook of Conducting Polymers*. 2nd ed. New York: Marcel Dekker; 1997.
14. Skotheim TA, Reynolds JR. *Handbook of Conducting Polymers*. 3rd ed. Boca Raton, FL: CRC Press; 2007.
15. Roncali J. Conjugated poly(thiophenes): synthesis, functionalization, and applications. *Chem Rev* 1992, 92:711–738.
16. Roncali J, Blanchard P, Frere P. 3,4-Ethylenedioxy thiophene (EDOT) as a versatile building block for advanced functional π-conjugated systems. *J Mater Chem* 2005, 15:1589–1610.
17. Huang H, Pickup PG. A donor-acceptor conducting copolymer with a very low band gap and high intrinsic conductivity. *Chem Mater* 1998, 10:2212–2216.
18. van Mullekom HAM, Vekemans JAJM, Meijer EW. Alternating copolymer of pyrrole and 2,1,3-benzothiadiazole. *Chem Commun* 1996:2163–2164.
19. Bijleveld JC, Zoombelt AP, Mathijssen SGJ, Wienk MM, Turbiez M, de Leeuw DM, Janssen RAJ. Poly(diketopyrrolopyrrole–terthiophene) for ambipolar logic and photovoltaics. *J Am Chem Soc* 2009, 131:16616–16617.
20. Havinga EE, ten Hoeve W, Wynberg H. Alternate donor-acceptor small-band-gap semiconducting polymers; polysquaraines and polycroconaines. *Synth Met* 1993, 55-57:299–306.
21. Chen J, Cao Y. Development of novel conjugated donor polymers for high-efficiency bulk-heterojunction photovoltaic devices. *Acc Chem Res* 2009, 42:1709–1718.
22. Shirota Y, Kageyama H. Charge carrier transporting molecular materials and their applications in devices. *Chem Rev* 2007, 107:953–1010.
23. Kittel C. *Introduction to Solid State Physics*. New York: John Wiley & Sons; 1976.
24. Fincher CR Jr, Ozaki M, Tanaka M, Peebles D, Lauchlan L, Heeger AJ. Electronic structure of polyacetylene: optical and infrared studies of undoped semiconducting $(CH)_x$ and heavily doped metallic $(CH)_x$. *Phys Rev B* 1979, 20:1589–1602.
25. Salzner U. Theoretical design of conducting polymers. *Curr Org Chem* 2004, 8:569–590.
26. Yang S, Olishevski P, Kertesz M. Bandgap calculations for conjugated polymers. *Synth Met* 2004, 141:171–177.
27. Hoffmann R. *Solids and Surfaces: A Chemist's View of Bonding in Extended Structures*. VCH: Weinheim; 1988.
28. Hoffmann R, Janiak C, Kollmar C. A chemical approach to the orbitals of organic polymers. *Macromolecules* 1991, 24:3725–3746.
29. Salaneck WR. Photoelectron spectroscopy of electrically conducting organic polymers. In: Skotheim TA, ed. *Handbook of Conducting Polymers*, vol. 2. New York: Marcel Dekker; 1986, 1337–1368.
30. Hill IG, Kahn A, Soos ZG, Pascal JRA. Charge-separation energy in films of π-conjugated organic molecules. *Chem Phys Lett* 2000, 327:181–188.
31. Cahen D, Kahn A. Electron energetics at surfaces and interfaces: concepts and experiments. *Adv Mater* 2003, 15:271–277.
32. Sato N, Seki K, Inokuchi H. Polarization energies of organic solids determined by ultraviolet photoelectron spectroscopy. *J Chem Soc, Faraday Trans II* 1981, 77:1621–1633.
33. Koopmans TA. Über die zuordnung von wellenfunktionen und eigenwerten zu den einzelnen elektronen eines atoms. *Physica* 1934, 1:104–113.

34. Refaely-Abramson S, Sharifzadeh S, Jain M, Baer R, Neaton JB, Kronik L. Gap renormalization of molecular crystals from density-functional theory. *Phys Rev B* 2013, 88:081204.
35. Ford WK, Duke CB, Paton A. The CNDO/S3 crystal orbital model: definition and application to polyacetylene. *J Chem Phys* 1982, 77:4564–4572.
36. Ford WK, Duke CB, Salaneck WR. Electronic structure of polypyrrole and oligomers of pyrrole. *J Chem Phys* 1982, 77:5030–5039.
37. Hill IG, Kahn A, Cornil J, dos Santos DA, Bredas JL. Occupied and unoccupied electronic levels in organic p-conjugated molecules: comparison between experiment and theory. *Chem Phys Lett* 2000, 317:444–450.
38. Kümmel S, Kronik L. Orbital-dependent density functionals: theory and applications. *Rev Mod Phys* 2008, 80:3–60.
39. Perdew JP, Parr RG, Levy M, Balduz JL. Density-functional theory for fractional particle number: derivative discontinuities of the energy. *Phys Rev Lett* 1982, 49:1691–1694.
40. Levy M, Perdew JP, Sahni V. Exact differential equation for the density and ionization energy of a many-particle system. *Phys Rev A* 1984, 30:2745.
41. Perdew JP, Norman MR. Electron removal energies in Kohn-Sham density-functional theory. *Phys Rev B* 1982, 26:5445.
42. Salzner U, Lagowski JB, Pickup PG, Poirier RA. Design of low band gap polymers employing density functional theory - hybrid functionals ameliorate the band gap problem. *J Comput Chem* 1997, 18:1943–1953.
43. Salzner U, Pickup PG, Poirier RA, Lagowski JB. Accurate method for obtaining band gaps in conducting polymers using a DFT/hybrid approach. *J Phys Chem A* 1998, 102:2572–2578.
44. Stowasser R, Hoffmann R. What do the Kohn-Sham orbitals and eigenvalues mean? *J Am Chem Soc* 1999, 121:3414–3420.
45. Choi CH, Kertesz M, Karpfen A. The effects of electron correlation on the degree of bond alternation and electronic structure of oligomers of polyacetylene. *J Chem Phys* 1997, 107:6712–6721.
46. Chong DP, Gritsenko OV, Baerends EJ. Interpretation of the Kohn-Sham orbital energies as approximate vertical ionization potentials. *J Chem Phys* 2002, 116:1760–1772.
47. Gritsenko OV, Baerends EJ. The analog of Koopmans' theorem in spin-density functional theory. *J Chem Phys* 2002, 117:9154–9159.
48. Kraisler E, Kronik L. Fundamental gaps with approximate density functionals: the derivative discontinuity revealed from ensemble considerations. *J Chem Phys* 2014, 140:18A540.
49. Perdew JP, Levy M. Physical content of the exact Kohn-Sham orbital energies: band gaps and derivative discontinuities. *Phys Rev Lett* 1983, 51:1884.
50. Iikura H, Tsuneda T, Yanai T, Hirao K. A long-range correction scheme for generalized-gradient-approximation exchange functionals. *J Chem Phys* 2001, 115:3540–3544.
51. Salzner U, Baer R. Koopmans' springs to life. *J Chem Phys* 2009, 131:231101–231104.
52. Tsuneda T, Song J-W, Suzuki S, Hirao K. On Koopmans' theorem in density functional theory. *J Chem Phys* 2010, 133:174101–174109.
53. Salzner U. Modeling photoelectron spectra of conjugated oligomers with time-dependent density functional theory. *J Phys Chem A* 2010, 114:10997–11007.
54. Salzner U, Aydin A. Improved prediction of properties of π-conjugated oligomers with range-separated hybrid density functionals. *J Chem Theory Comput* 2011, 7:2568–2583.
55. Livshits E, Baer R. A well-tempered density functional theory of electrons in molecules. *Phys Chem Chem Phys* 2007, 9:2932–2941.
56. Baer R, Livshits E, Salzner U. Tuned range-separated hybrids in density functional theory. *Annu Rev Phys Chem* 2010, 61:85–109.
57. Kronik L, Stein T, Refaely-Abramson S, Baer R. Excitation gaps of finite-sized systems from optimally tuned range-separated hybrid functionals. *J Chem Theory Comput* 2011, 8:1515–1531.
58. Refaely-Abramson S, Baer R, Kronik L. Fundamental and excitation gaps in molecules of relevance for organic photovoltaics from an optimally tuned range-separated hybrid functional. *Phys Rev B* 2011, 84:075144.
59. Stein T, Autschbach J, Govind N, Kronik L, Baer R. Curvature and frontier orbital energies in density functional theory. *J Phys Chem Lett* 2012, 3: 3740–3744.
60. Körzdörfer T, Kümmel S, Marom N, Kronik L. When to trust photoelectron spectra from Kohn-Sham eigenvalues: the case of organic semiconductors. *Phys Rev B* 2009, 79:201205.
61. Runge R, Gross EKU. Density-functional theory for time-dependent systems. *Phys Rev Lett* 1984, 52:997–1000.
62. Bauernschmitt R, Ahlrichs R. Treatment of electronic excitations within the adiabatic approximation of time dependent density functional theory. *Chem Phys Lett* 1996, 256:454–464.
63. Casida ME, Jamorski C, Casida KC, Salahub DR. Molecular excitation energies to high-lying bound states from time-dependent density-functional response theory: characterization and correction of the time-dependent local density approximation ionization threshold. *J Chem Phys* 1998, 108:4439–4449.
64. Stratmann RE, Scuseria GE, Frisch MJ. An efficient implementation of time-dependent density-functional

theory for the calculation of excitation energies of large molecules. *J Chem Phys* 1998, 109: 8218–8224.

65. Chai J-D, Head-Gordon M. Long-range corrected hybrid density functionals with damped atom-atom dispersion corrections. *Phys Chem Chem Phys* 2008, 10:6615–6620.
66. da Silva Filho DA, Coropceanu V, Fichou D, Gruhn NE, Bill TG, Gierschner J, Cornil J, Bredas J-L. Hole-vibronic coupling in oligothiophenes: impact of backbone torsional flexibility on relaxation energies. *Philos Trans Roy Soc A* 2007, 365:1435–1452.
67. Frisch MJ, Trucks GW, Schlegel HB, Scuseria GE, Robb MA, Cheeseman JR, Scalmani G, Barone V, Mennucci B, Petersson GA, et al. Gaussian 09, Revision A.1. 2009.
68. Salzner U, Karalti O, Durdagi S. Does the donor-acceptor concept work for designing synthetic metals? III. Theoretical investigation of copolymers between quinoid acceptors and aromatic donors. *J Mol Model* 2006, 12:687–701.
69. Kuhn H. A quantum-mechanical theory of light absorption of organic dyes and similar compounds. *J Chem Phys* 1949, 17:1198–1212.
70. Kutzelnigg W. Zur behandlung der bindungsalter nierung als störung in der hückelschen MO-theorie. *Theor Chim Acta* 1966, 4:417–433.
71. Kertesz M, Choi CH, Yang S. Conjugated polymers and aromaticity. *Chem Rev* 2005, 105:3448–3481.
72. Zade SS, Zamoshchik N, Bendikov M. From short conjugated oligomers to conjugated polymers. Lessons from studies on long conjugated oligomers. *Acc Chem Res* 2011, 44:14–24.
73. Granville MF, Holtom GR, Kohler BE. High-resolution one and two photon excitation spectra of *trans, trans*-1,3,5,7-octatetraene. *J Chem Phys* 1980, 72:4671–4675.
74. Gavin RM Jr, Weisman C, McVey JK, Rice SA. Spectroscopic properties of polyenes. III 1,3,5,7-octatetraene. *J Chem Phys* 1978, 68:522–529.
75. D'Amico KL, Manos C, Christensen RL. Electronic energy levels in a homologues series of unsubstituted linear polyenes. *J Am Chem Soc* 1980, 102:1777–1782.
76. Dierksen M, Grimme S. Density functional calculations of the vibronic structure of electronic absorption spectra. *J Chem Phys* 2004, 120:3544–3554.
77. Gierschner J, Cornil J, Egelhaaf HJ. Optical bandgaps of π-conjugated organic materials at the polymer limit: experiment and theory. *Adv Mater* 2007, 19: 173–191.
78. Sonmez G, Shen CKF, Rubin Y, Wudl F. A red, green, and blue (RGB) polymeric electrochromic device (PECD): the dawning of the PECD era. *Angew Chem Int Ed Engl* 2004, 43:1498–1502.
79. Jespersen KG, Beenken WJD, Zaushisyn Y, Yartsev A, Andersson M, Pullerits T, Sundström V. The electric states of polyfluorene coploymers with alternating donor-acceptor units. *J Chem Phys* 2004, 121:12613–12617.
80. Hung Y-C, Jiang J-C, Chao C-Y, Su W-F, Lin S-T. Theoretical study on the correlation between band gap, bandwidth, and oscillator strength in fluorene-based donor-acceptor conjugated copolymers. *J Phys Chem B* 2009, 113:8268–8277.
81. Kuhn W. Über die gesamtstarke der von einem zustande ausgehenden absorptionslinien. *Z Phys* 1925, 33:408–412.
82. Salzner U, Köse ME. Does the donor-acceptor concept work for designing synthetic metals? 2. theoretical investigation of copolymers of 4-(dicyanomethylene-4*h*-cyclopenta[2,1-*b*:3,4-*b*′]dithiophene and 3,4-(ethylenedioxy)thiophene. *J Phys Chem B* 2002, 106:9221–9226.
83. Kanimozhi C, Yaacobi-Gross N, Chou KW, Amassian A, Anthopoulos TD, Patil S. Diketopyrrolopyrrole–diketopyrrolopyrrole-based conjugated copolymer for high-mobility organic field-effect transistors. *J Am Chem Soc* 2012, 134:16532–16535.
84. Li Y. Molecular design of photovoltaic materials for polymer solar cells: toward suitable electronic energy levels and broad absorption. *Acc Chem Res* 2012, 45:723–733.
85. Güneş S, Neugebauer H, Sariçiftci NS. Conjugated polymer-based organic solar cells. *Chem Rev* 2007, 107:1324–1338.
86. Naarmann CH, Theophilou N. New process for the production of metal-like, stable polyacetylene. *Synth Met* 1987, 22:1–8.
87. Roncali J, Yassar Y, Garnier F. Electrosynthesis of highly conducting poly(3-methylthiophene) thin films. *J Chem Soc Chem Commun* 1988:581–582.
88. Qi G, Huang L, Wang H. Highly conductive free standing polypyrrole films prepared by freezing interfacial polymerization. *Chem Commun* 2012, 48:8246–8248.
89. Pople JA, Walmsley SH. Bond alternation defects in long polyene molecules. *Mol Phys* 1962, 5: 15–20.
90. Su WP, Schrieffer JR, Heeger AJ. Soliton excitations in polyacetylene. *Phys Rev B* 1980, 22:2099–2111.
91. Campbell DK, Bishop AR, Fesser K. Polarons in quasi-one-dimensional systems. *Phys Rev B* 1982, 26:6862–6974.
92. Scott JC, Pfluger P, Krounbi MT, Street GB. Electron-spin-resonance studies of pyrrole polymers: evidence for bipolarons. *Phys Rev B* 1983, 28:2140.
93. Brédas JL, Street GB. Polarons, bipolarons, and solitons in conducting polymers. *Acc Chem Res* 1985, 18:309–315.

94. Walker CT, Slack GA. Who named the—ONs? *Am J Phys* 1970, 38:1380–1389.
95. Fisher AJ, Hayes W, Wallace DS. Polarons and solitons. *J Phys Condens Matter* 1989, 1:5567–5593.
96. Scott JC, Brédas JL, Yakushi K, Pfluger P, Street GB. The evidence for bipolarons in pyrrole polymers. *Synth Met* 1984, 9:165–172.
97. Chung T-C, Kaufman JH, Heeger AJ, Wudl F. Charge storage in doped poly(thiophene): optical and electrochemical studies. *Phys Rev B* 1984, 30: 702–710.
98. Fesser K, Bishop AR, Campbell DK. Optical absorption from polarons in a model of polyacetylene. *Phys Rev B* 1983, 27:4804–4825.
99. Fichou D, Horowitz G, Xu B, Garnier F. Stoichiometric control of the successive generation of the radical cation and dication of extended α-conjugated oligothiophenes: a quantitative model for doped polythiophene. *Synth Met* 1990, 39:243–259.
100. Furukawa Y. Reexamination of the assignments of electronic absorption bands of polarons and bipolarons in conducting polymers. *Synth Met* 1995, 69:629–632.
101. Furukawa Y. Electronic absorption and vibrational spectroscopies of conjugated polymers. *J Phys Chem* 1996, 100:15644–15653.
102. van Haare JAEH, Havinga EE, van Dongen JLJ, Janssen RAJ, Cornil J, Brédas JL. Redox states of long oligothiophenes: two polarons on a single chain. *Chem Eur J* 1998, 4:1509–1522.
103. Zaikowski L, Kaur P, Gelfond C, Selvaggio E, Asaoka S, Wu Q, Chen H-C, Takeda N, Cook AR, Yang A, et al. Polarons, bipolarons, and side-by-side polarons in reduction of oligofluorenes. *J Am Chem Soc* 2012, 134:10852–10863.
104. Bakalis J, Cook AR, Asaoka S, Forster M, Scherf U, Miller JR. Polarons, compressed polarons, and bipolarons in conjugated polymers. *J Phys Chem C* 2014, 118:114–125.
105. Heeger AJ, Kivelson S, Schrieffer JR, Su W-P. Solitons in conducting polymers. *Rev Mod Phys* 1988, 60:781–850.
106. Boudreaux DS, Chance RR, Brédas JL, Silbey R. Solitons and polarons in polyacetylene: self-consistent-field calculations of the effect of neutral and charged defects on molecular geometry. *Phys Rev B* 1983, 28:6927–6936.
107. Brocks G. Polarons and bipolarons in oligothiophenes: a first principles study. *Synth Met* 1999, 102:914–915.
108. Brocks G. π-Dimers of Oligothiophene Cations. *J Chem Phys* 2000, 112:5353–5363.
109. Del Re G, Ladik J, Bizco G. Self-consistent-field tight-binding treatment of polymers. I. Infinite three-dimensional case. *Phys Rev* 1967, 155: 997–1003.
110. Brédas J-L. Electronic Structure of Highly Conducting Polymers. In: Skotheim TA, ed. *Handbook of Conducting Polymers*. New York: Marcel Dekker; 1986, 859–913.
111. Ladik J. *Quantum Theory of Polymers as Solids*. New York: Plenum Press; 1988.
112. Suhai S. Quasiparticle energy-band structures in semiconducting polymers: correlation effects on the band gap in polyacetylene. *Phys Rev B* 1983, 27:3506–3518.
113. Bally T, Hrovat DA, Thatcher Borden W. Attempts to model neutral solitons in polyacetylene by *ab initio* and density functional methods. The nature of the spin distribution in polyenyl radicals. *Phys Chem Chem Phys* 2000, 2:3363–3371.
114. Dreuw A, Head-Gordon M. Single-reference ab initio methods for the calculation of excited states of large molecules. *Chem Rev* 2005, 105:4009–4037.
115. Bally T, Sastry GN. Incorrect dissociation behavior of radical ions in density functional calculations. *J Phys Chem A* 1997, 101:7923–7925.
116. Cohen AJ, Mori-Sanchez P, Yang W. Insights into current limitations of density functional theory. *Science* 2008, 321:792–794.
117. Vogl P, Campbell DK. First-principles calculations of the three-dimensional structure and intrinsic defects in trans-polyacetylene. *Phys Rev B* 1990, 41:12797–12817.
118. Salzner U. Theoretical investigation of excited states of large polyene cations as model systems for lightly doped polyacetylene. *J Chem Theory Comput* 2007, 3:219–231.
119. Salzner U. Theoretical investigation of excited states of oligothiophenes and of their monocations. *J Chem Theory Comput* 2007, 3:1143–1157.
120. Zade SS, Bendikov M. Theoretical study of long oligothiophene polycations as a model for doped polythiophene. *J Phys Chem C* 2007, 111:10662–10672.
121. Alkan F, Salzner U. Theoretical investigation of excited states of oligothiophene anions. *J Phys Chem A* 2008, 112:6053–6058.
122. Salzner U. Investigation of charge carriers in doped thiophene oligomers through theoretical modeling of their UV/Vis spectra. *J Phys Chem A* 2008, 112:5458–5466.
123. Zamoshchik N, Salzner U, Bendikov M. Nature of charge carriers in long doped oligothiophenes. The effect of counterions. *J Phys Chem C* 2008, 112:8408–8418.

FURTHER READING/RESOURCES

Lehmann CW. Crystal structure prediction—the dawn of a new era. *Angew Chem* 2011, 50:5616–5617.

Salzner U. Conjugated organic polymers: from bulk to molecular wire. In: Rieth M, Schommers W, eds. *Handbook of Theoretical and Computational Nanotechnology*, vol. 8. Los Angeles, CA: ASP; 2006, 203–251.

Scharber MC, Mühlbacher D, Koppe M, Denk P, Waldauf C, Heeger AJ, Brabec C. Design rules for donors in bulk-heterojunction solar cells—towards 10% energy-conversation efficiency. *Adv Mater* 2006, 18:789–794.

Takimiya K, Osaka I, Nakano M. π-Building blocks for organic electronics: revaluation of "inductive" and "resonance" effects of π-electron deficient units. *Chem Mater* 2014, 26:587–593.